Visualization Problems of a Supersonic Tip Vortex in a Heat Wake

T.V. Konstantinovskaya[1], V.E. Borisov[2], A.E. Lutsky[3]

Keldysh Institute of Applied Mathematics RAS

[1] ORCID: 0000-0002-1127-503X, konstantinovskaya.t.v@gmail.com
[2] ORCID: 0000-0003-4448-7474, narelen@gmail.com
[3] ORCID: 0000-0002-4442-0571, allutsky@yandex.ru

Abstract

Scientific visualization is certainly a very important and useful area of research, providing utilities not only for visualization, but also for the investigation and analysis of the data obtained. Herewith, the data can be both experimental and numerical.

This paper demonstrates the application of scientific visualization and identification methods of vortex structures to the problem of the supersonic tip vortex propagation in the incoming flow disturbed by an energy source. The undisturbed incoming flow Mach number was $M_\infty = 3$, the wing attack angle was 10°. Numerical data were obtained in the region of 30 wing chords downstream from the wing axis.

At the same time, significant differences are shown between the results of applying classical visualization methods, such as λ_2 and Q, and the third-generation *Liutex* method to the considered problem for visualization and identification of the tip vortex. Moreover, according to the results of further research, it seems that a more truthful picture of the flow is given by the method of the third generation while used classical methods give false additional vortex data.

Numerical simulations were performed with the developed ARES software package for modeling 3D turbulent flows on high-performance computer systems on the hybrid supercomputer system K-60 at the Keldysh Institute of Applied Mathematics of the Russian Academy of Sciences. 112 processors were used for perform the simulations.

Keywords: supersonic flow, energy wake, tip vortex identification, scientific visualization tools.

1. Introduction

Under normal conditions, the flow around an aircraft is accompanied by the formation of various vortex structures. They have a significant impact on the aerodynamics and efficiency of aircraft control elements, up to a complete loss of control. A special case is represented by such vortex structures as tip vortices. They accompany the flight of any aircraft, breaking off from its various elements: the edges of the wings, controls, finned parts of the fuselage. The properties of tip vortices and their interaction with various objects have been actively studied since the middle of the XX century.

For subsonic flight modes, the main attention was paid to the safety of aircraft operation, in particular, the safety of airports. Indeed, an aircraft that caught in the vortex wake of a leading aircraft suffers an intense circular moment, which can lead to an arbitrary change in course, altitude, etc [1]. In such situations, even a complete loss of control can occur. This can be especially critical at low speeds and altitude, especially in conditions of flying aircraft heavy traffic – and this is the standard operating conditions of airports. In world practice, both abnormal and catastrophic situations are known, the main cause of which was the described phenomenon [2]. There are the other risks in addition to the risk of getting into the

wake of the aircraft in frontward for supersonic flight modes. Namely, the risks of getting a tip vortex on other elements of the aircraft located downstream (including control system elements), as well as its possible entry into the combustion chamber of the propulsion system become relevant. Such situations can also cause loss of control, especially in the case of supersonic modes. Taking into account the newly increased interest in supersonic aircraft in both the military and civilian industries, the study of supersonic vortices remains an important and topical task of aerodynamics.

Scientific visualization methods help not only to visualize the flow, but may be effectively used as data analysis tools because they serve not only for visualization, but also allow to distinguish its main structures, to compare them, etc. This undoubtedly useful property makes from scientific visualization methods a useful tool for scientists around the world. The corresponding reviews can be found, for example, in [3-6].

As a rule, the properties of tip vortices are studied in the case of a homogeneous incoming flow. Despite the fact that there are studies on the influence of disturbances on the tip vortex in subsonic modes, in the case of supersonic flow the influence of disturbances remains an almost unexplored problem. The problem of the presence of an energy source upstream the wing generator is considered in the work as a special case of the incoming flow disturbance.

2. Problem Statement
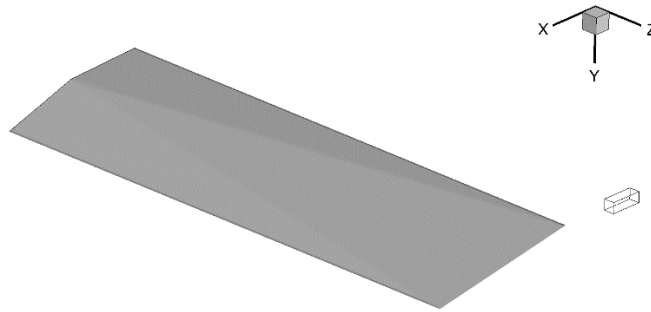
Figure 1. General model scheme: wing generator and energy source zone

The supersonic flow around a wing with an energy source upstream from the wing leading edge was studied (Fig. 1). Namely, the influence of the energy source on the formation and propagation of the tip vortex from the tip edge of the wing generator was investigated. The energy input area had the form of a parallelepiped with the coordinates of the corner points $(x_1, y_1, z_1) = (-0.031, -0.0036, 0.094)$ and $(x_2, y_2, z_2) = (-0.025, -0.0016, 0.096)$. Thus, it was located in the upward flow direction symmetrically relative to the intersection point of the leading and tip edges of the wing at a distance of about a third of the wing chord from its leading edge, as shown in Fig. 1. The Mach number of the incoming flow was $M_\infty = 3$. The simulations were performed in dimensionless variables [7], a unit of length was taken $L = 1$ m. Density and pressure were non-dimensionalized by its free stream values. The Reynolds number was $Re_L = 10^7$. The wing generator was a straight half-wing, rectangular in plan, with sharp leading, tip and trailing edges. The wing had a diamond-shaped base with a thickness of 13.3% of the wing chord. The wing had a half-span $l = 0.095$, a chord $b = 0.03$.

The x axis was co-directed to the sense of incoming flow. The z axis coincided with the wing axes. The y axis was directed from the leeward side of the wings to the windward side. The length of the numerical domain under consideration exceeded 30 wing chords downstream from the wing axes.

3. Numerical Model

A system of unsteady Favre averaged Navier–Stokes equations (URANS) was used to describe the three-dimensional turbulent flow of a compressible gas. The hybrid DES method

(detached eddy simulation) realized on the basis of the Spalart-Allmaras (SA) turbulence model by modification of the linear scale of turbulence was used [8].

The approximation of the model equations in space was carried out using the finite volume method with a TVD reconstruction scheme of the 2nd order of accuracy. Assuming that the computational domain is covered by a grid consisting of non-overlapping polyhedral cells, the finite volume method is implemented by integrating a system of model equations for each cell with following transformation of volume integrals from fluxes into surface integrals over the cell faces. A generalized Godunov method with exact Riemannian solver was used to calculate inviscid fluxes on the faces of the numerical cells. Both explicit and implicit (based on the LU-SGS method) schemes were used to approximate the equations in time (depending on the series of simulations). The used numerical method is described in [9].

A software package ARES for parallel computing developed at the Keldysh Institute of Applied Mathematics of the Russian Academy of Sciences was used for numerical simulations [10]. The simulations were carried out on the K-60 hybrid supercomputer system [11] using 112 numerical cores. The mesh consisted of 15,296,688 cells. The mesh was refined in the zones of vortex formation and propagation in order to better resolution of vortex structures.

4. Visualization of flow vortex structures

A separate module for determining vortex structures on hexagonal grids in the form of postprocessing treatment was implemented within the software package ARES used for simulations. Within its framework, some classical methods of scientific visualization, such as the λ_2, Q method, etc., are fully implemented. The implementation of the *Liutex* method of scientific visualization - the latest generation method for determining vortex structures - also added. The module generates output data in the format of the Tecplot software package.

4.1. λ_2 visualization method

The λ_2 method (or criterion) is quite widespread and is often used in data processing for the identification of vortex structures. It was proposed in [12]. According to this criterion, the vortex flow region identification is based on the analysis of the eigenvalues of the symmetric matrix
$\mathbf{A} = \mathbf{S}^2 + \mathbf{\Omega}^2$, which are always real. Here $\mathbf{S}$ and $\mathbf{\Omega}$, respectively, are strain rate and vorticity tensors of the flow):

$$\nabla\mathbf{u} = \mathbf{S} + \mathbf{\Omega}, \quad S_{i,j} = \frac{1}{2}\left(\frac{\partial u_i}{\partial x_j} + \frac{\partial u_j}{\partial x_i}\right), \quad \Omega_{i,j} = \frac{1}{2}\left(\frac{\partial u_i}{\partial x_j} - \frac{\partial u_j}{\partial x_i}\right),$$

where $\nabla\mathbf{u}$ is the flow velocity gradient tensor.

According to the method, the vortex region is considered to be the part of space in which the second eigenvalue is negative $\lambda_2(\mathbf{A}) < 0$ $(\lambda_1 \geq \lambda_2 \geq \lambda_3)$.

4.2. Q visualization method

The Q method (criterion) as well as the λ_2 method, is expressed in terms of the matrices $\mathbf{S}$ (strain rate tensor) and $\mathbf{\Omega}$ (vorticity tensor) and under the assumption of incompressible flow has the form [13]:

$$Q = \frac{1}{2}(\|\mathbf{\Omega}\|^2 - \|\mathbf{S}\|^2)$$

that is a measure of how much the local rotation velocity exceeds the local deformation degree. Thus, the vortex region is determined at $Q > 0$.

4.3. *Liutex* visualization method

The *Liutex* method (criterion) for visualization of vortex structures is one of the latest – it's a third-generation method, free from shear and compressive components of the strain rate tensor by its construction [14]. It allows to evaluate not only the direction, but also the strength of the vortex.

The method was published in 2018 as *Rortex* [15], later it was renamed *Liutex* after one of the authors [16].

According to this criterion, the flow domain with vortex structures is that where the strain rate tensor has one real λ_r and two complex conjugate eigenvalues. Using these eigenvalues, the Rotex vector [12] is determined:

$$\mathbf{R} = \mathcal{R}\,\mathbf{r}, \quad \mathcal{R} = \boldsymbol{\omega}\cdot\mathbf{r} - \sqrt{(\boldsymbol{\omega}\cdot\mathbf{r})^2 - 4\lambda_{ci}^2},$$

where $\boldsymbol{\omega}$ – vorticity vector, $\mathbf{r}$ – normalized eigenvector corresponding to the λ_r with condition $\boldsymbol{\omega}\cdot\mathbf{r} > 0$. It locally coincides with the axis of rotation of the vortex as a solid body. Based on it, a normalized value $\Omega_R \in [0,1]$ is formed which shows the intensity of the flow local rotation:

$$\Omega_R = \frac{\left(\boldsymbol{\omega}\cdot\mathbf{r}\right)^2}{2\left[\left(\boldsymbol{\omega}\cdot\mathbf{r}\right)^2 - 2\lambda_{ci}^2 + 2\lambda_{cr}^2 + \lambda_r^2\right] + \varepsilon_{Lu}}, \quad \varepsilon_{Lu} = k\max\{\lambda_{ci}^2\}.$$

Here ε_{Lu} is the value intended for filtering of numerical "noise", the maximum is taken over the entire domain under consideration, $k = 0.001 \sim 0.002$ [12, 13].

5. Results and visualization

The obtained study and visualization results of the supersonic flow around the wing disturbed by energy source in front of its leading edge are presented in this part of the paper (Fig. 1).

When an energy source is added to the flow, a heat wake is formed behind it. The heat wake is characterized by such changes in the main characteristics as reduced pressure (*P*) and density (*R*) and increased temperature (*T*) (Fig. 2). Thus, instead of a uniform incoming flow, a stream with an area of changed basic parameters flows around the wing, which is shown in Fig. 3. It shows the distribution of parameters in the cross-section directly before the leading edge of the generator wing – at coordinate $x = -0.0175$ (at a distance of about 1/12 of the wing chord upward from wing leading edge). Temperature in undisturbed incoming flow equals to 1 and in the heat wake before wing it reaches value of 7.5.
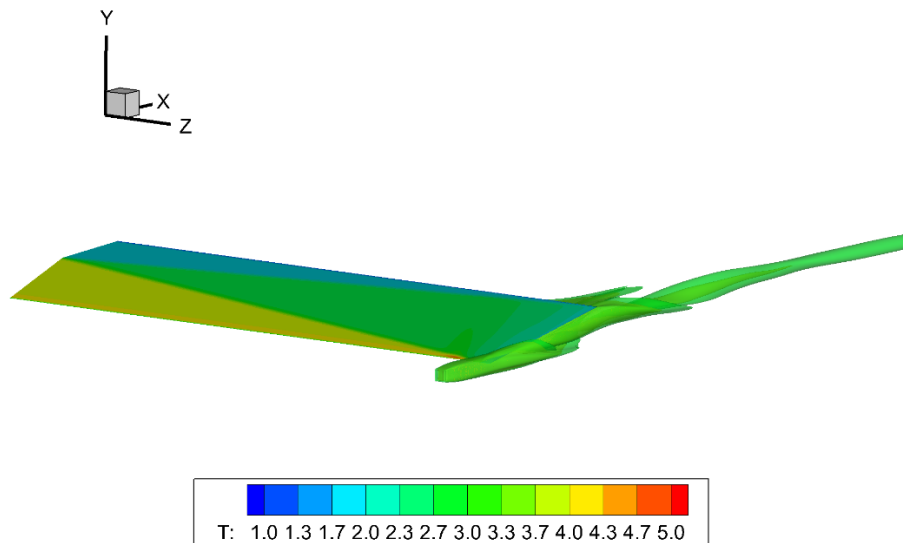
Figure 2. Heat wake from energy source coming to the wing. Wing is colored by pressure
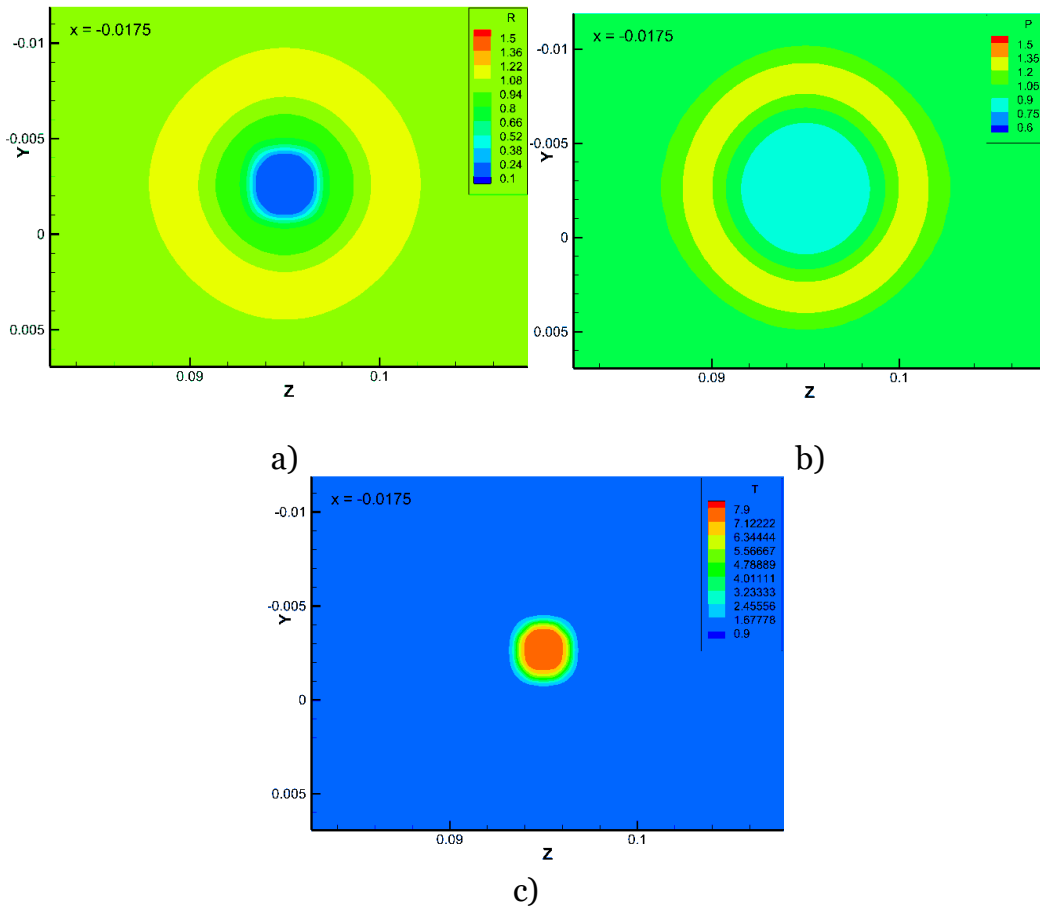
Figure 3. Gas dynamic functions distribution in the cross-section at x = -0.0175 in the incoming flow disturbed by energy source: a) density R, b) pressure P, c) temperature T

The supersonic tip vortex undergoes changes when it is being in a perturbed incoming flow compared with unperturbed one. In confirmation of this fact we present the density distribution in a longitudinal section z = 0.093 closing to the vortex axis for an unperturbed (Fig. 4-a) and perturbed by energy source (Fig. 4-b) incoming flow. Density change is obvious under the influence of a heat wake: the density values in the vortex core decrease with the simultaneous expansion of the low density region, which is especially noticeable in the vortex near zone and the vortex formation zone.
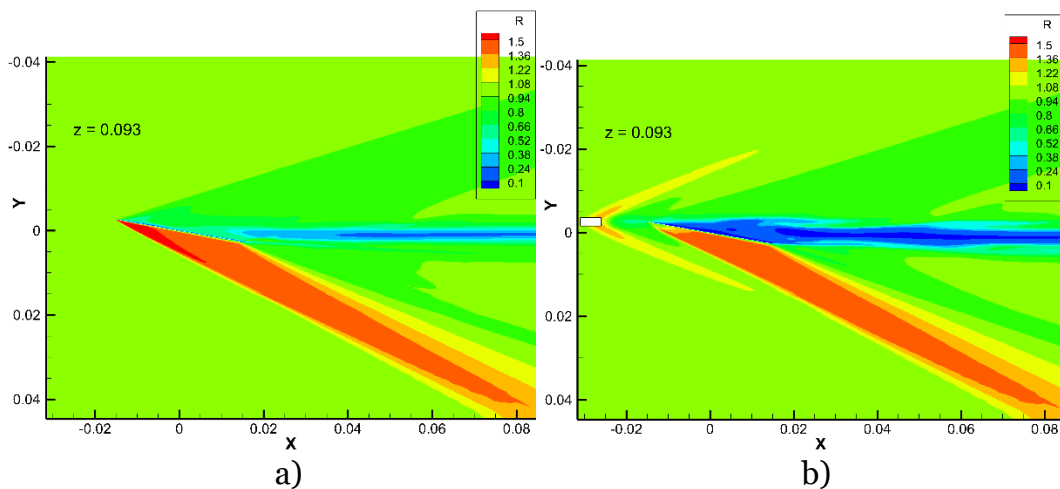
Figure 4. Density distribution (R) in longitudinal section z = 0.093: a) undisturbed incoming flow, b) disturbed by energy source incoming flow

When the incoming supersonic flow is perturbed by an energy source, in addition to density decrease on the vortex axis, a second local minimum of density R appears, which is shown in the cross section $x = 0.1$ in Fig. 5. A decrease in the density values on the vortex axis in the presence of an energy source is observed throughout the all considered region (Fig. 6). The vortex axis vorticity increases in the presence of an energy source (Fig. 7). This indicates an increase in the intensity of the vortex, because the more of the vortex parameters differ from the free flow, the more vortex is intensive. There are no significant changes in the values of the tangential Mach number M_{yz} in the vortex core when it affected by a heat wake (Fig. 7). However, there is a change in the shape of the distribution of this parameter, in which a greater value passes from the wing tip chord side to the wing root chord side. Further researches are worthwhile for a broader understanding of the flow pattern.

a)   b)
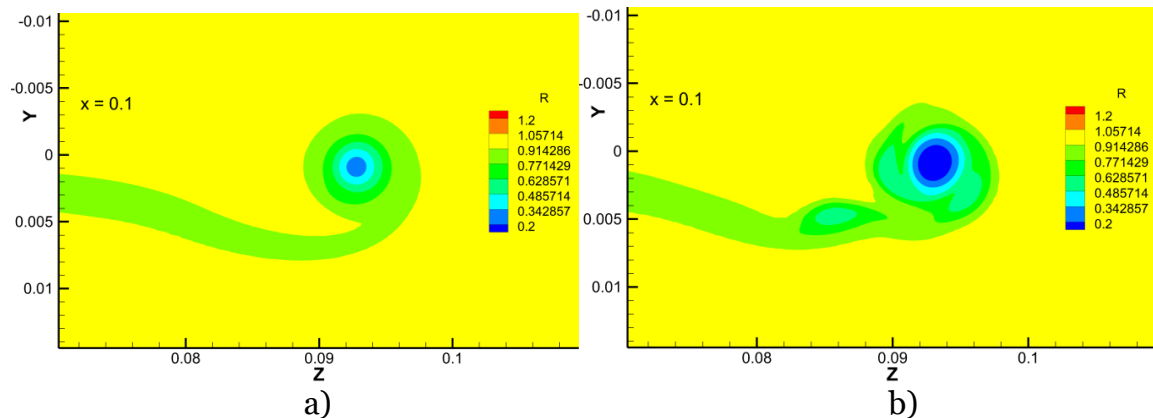
Figure 5. Density distribution (R) in the cross section $x = 0.1$ for: a) undisturbed incoming flow, b) incoming flow with an energy source
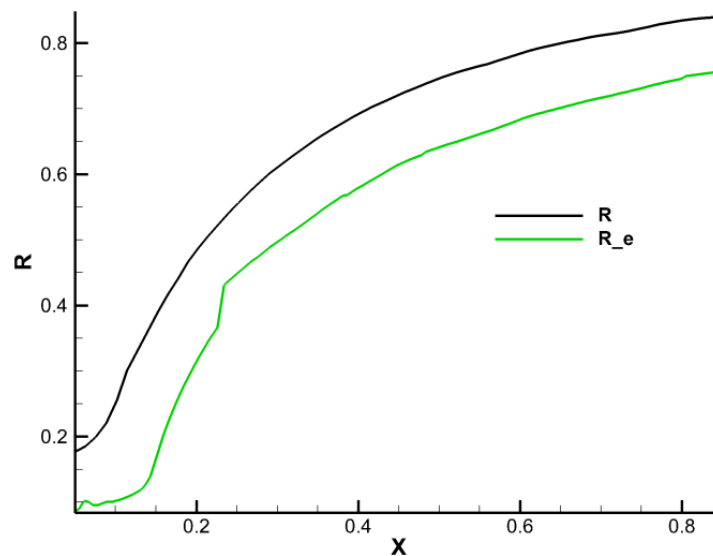
Figure 6. The density value (R) on the tip vortex axis in an undisturbed flow (black) and in energy source disturbance (green)
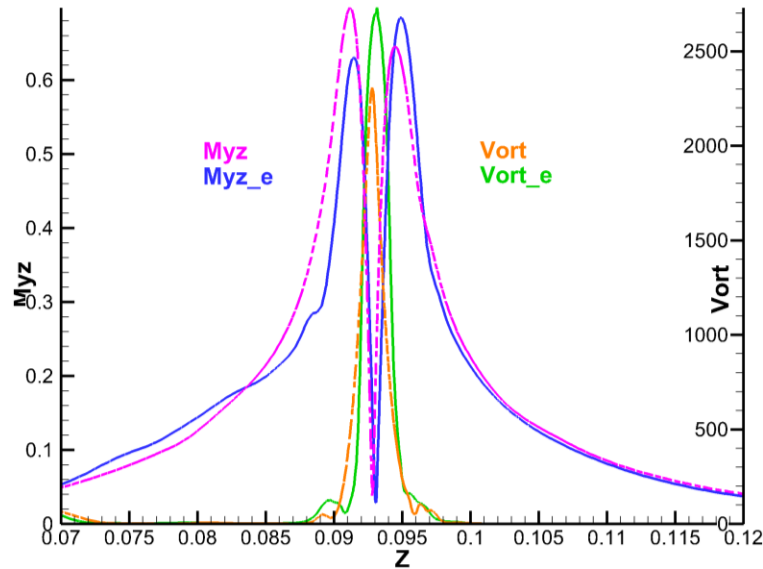
Figure 7. Tangential Mach number M_{yz} and vorticity *Vort* along the line passing through the vortex axis in the cross-section $x = 0.1$ in an undisturbed flow (dashed) and in energy source disturbance (solid)

The methods of vortex structures scientific visualization described in section 4 (λ_2, Q and *Liutex*) were applied to the considered problem of the supersonic tip vortex propagation in the upward presence of an energy source. By traditional methods (λ_2 and Q), a bifurcation of the tip vortex was obtained in the near region behind the wing (Fig. 8). According to these methods, the double vortex propagates to the value $x = 0.265$, which corresponds to 8.83 wing chords downstream the wing axis. Then the two its parts merge, forming one main vortex. Fig. 8 shows the results of visualization with the following parameter values: $\lambda_2 = -1000$ (orange) and $Q = 1000$ (blue); a) in the near field, b) in the entire calculation area.

A more detailed study shows that a small additional vortex structure is observed directly behind the wing in the place where the second vortex is determined by classical methods. This can be seen in Fig. 9-a, where the density distribution and stream traces in the cross section $x = 0.03$ are shown. However, already at a distance of slightly less than one wing chord from the wing trailing edge (at $x = 0.04$), only one main structure of the tip vortex is observed (Fig. 9-b), and further downstream, second vortex does not appear in this location. This does not correspond to the application results of classical visualization methods λ_2 and Q which define two vortex structures at these distances downstream the wing. Additional vortex structures directly behind the wing trailing edge are associated to a greater extent with the vortex formation zone.

Figure 10 shows the application result of vortex visualization *Liutex* criterion at $\tilde{\Omega}_R = 0.45$. According to the *Liutex* criterion, several vortex structures are determined in the cross section $x = 0.03$, including the same second vortex that is shown in Fig. 11-a by red lines that correspond to the value of $\tilde{\Omega}_R = 0.4$. At the same time the value of $\tilde{\Omega}_R = 0.45$ no longer shows such an insignificant vortex structure (Fig. 11-b). Starting from the value $x = 0.05$ (which corresponds to 1.166 chords downstream the trailing edge), according to the *Liutex* criterion, only one vortex structure is observed - a tip vortex, which corresponds to the flow pattern (Fig. 12). Figure 12 shows the density distribution R and level lines $\tilde{\Omega}_R = 0.45$ at cross-sections $x = 0.04$ and $x = 0.05$.
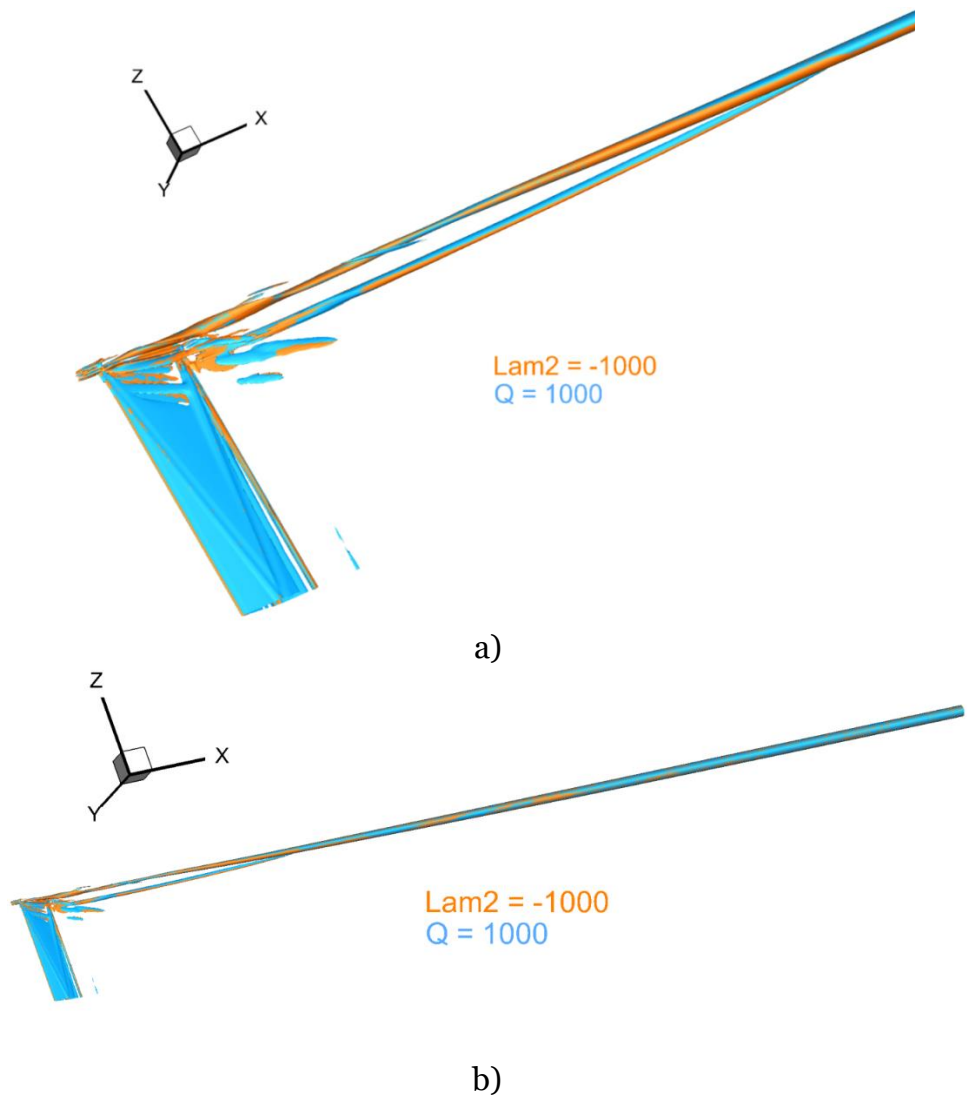
Figure 8. The application result of the scientific visualization traditional methods λ_2 and Q: a) in the near field, b) in the entire computational domain. The isosurfaces λ_2 = -1000 (orange) and Q = 1000 (blue) are shown
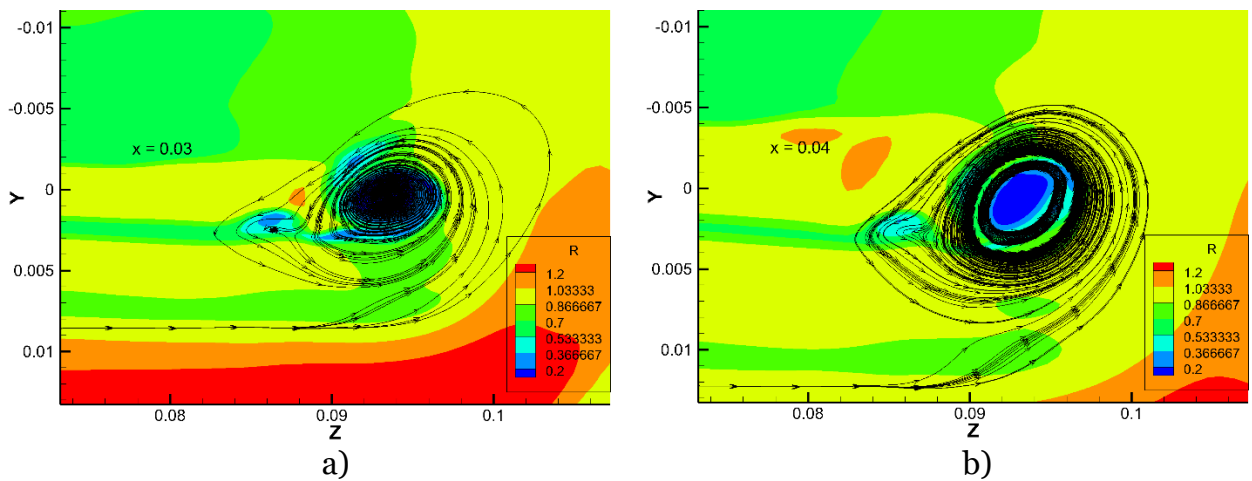
Figure 9. Density distribution R and stream traces in cross-sections: a) x = 0.03, b) x = 0.04
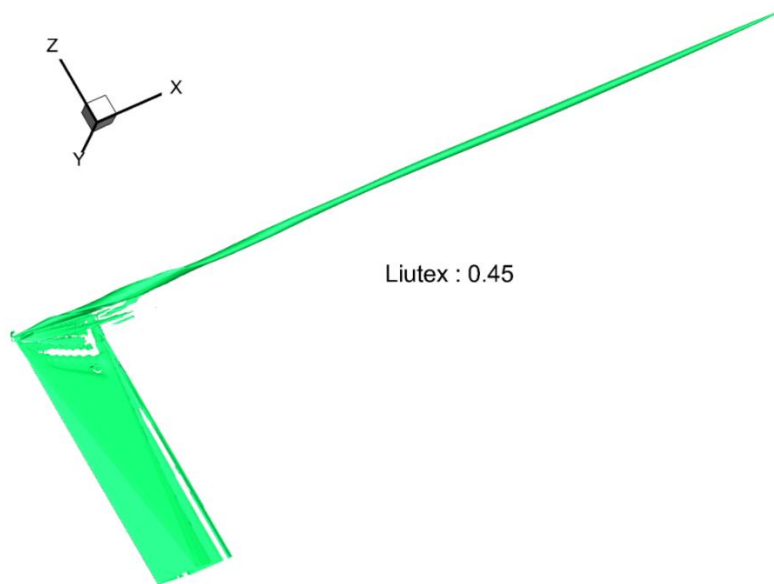
Figure 10. Application result of *Liutex* criterion of vortex identification, $\widetilde{\Omega}_R = 0.45$

Thus, traditional methods of vortex structures identification and visualization respond to the density gradient, namely to the second local minimum of density, defining a second "vortex" at this aria. Unlike the *Liutex* method which in this problem does not show a second vortex in the region of the second local density minimum.
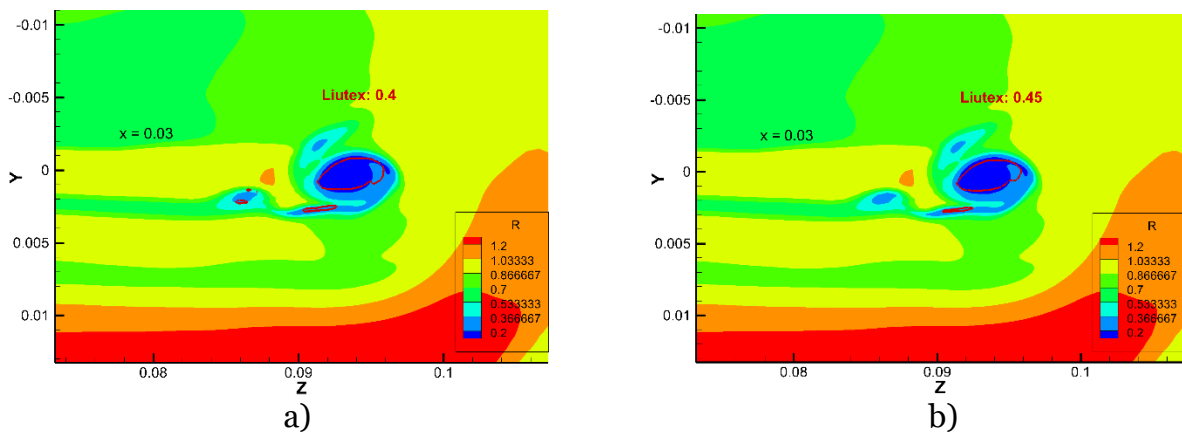
Figure 11. Density distribution R and level lines of *Liutex* criterion in cross-section $x = 0.03$: a) $\widetilde{\Omega}_R = 0.4$, b) $\widetilde{\Omega}_R = 0.45$
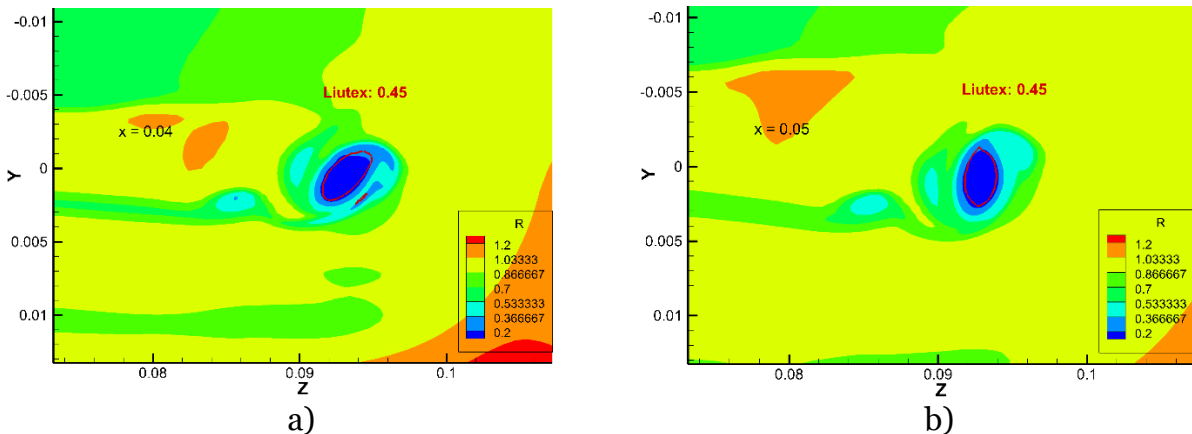
Figure 12. Density distribution R and level lines of *Liutex* criterion $\widetilde{\Omega}_R = 0.45$ in cross-sections: a) $x = 0.04$, b) $x = 0.05$

6. Conclusion

The paper presents the results of analysis and scientific visualization of the supersonic tip vortex propagation problem in the incoming flow disturbed by an energy source in front of the leading edge of the generator wing. The Mach number of the undisturbed incoming flow was $M_\infty = 3$, the angle of attack of the wing generator was 10°.

The numerical simulations were performed by the author's ARES software package, within which the used visualization methods are implemented as a post-processing module, where the output data is generated in the format of the Tecplot software package.

Scientific visualization methods allow not only to visualize the obtained data, but also to effectively analyze them. However, it is necessary to pay more attention to the limitations associated with the use of a particular method of scientific visualization, taking into account the pros and cons of each of them.

Thus, for the considered supersonic problem (with an energy source), it was found that classical methods of vortex structures visualization and identification, such as λ_2 and Q, give an incorrect idea of the flow, namely, its implication determines the bifurcation of the tip vortex in the near zone (up to 8.83 chords of the wing downstream the wing axis). This is refuted by additional studies that show that one tip vortex is observed after the formation zone (bounded by one chord downstream the wing trailing edge), which is characterized by multiple vortex structures and by active influence of the wing veil.

However, the application of the vortex structures identification method of the third generation the *Liutex* criterion gives as a result one vortex starting from the distance of about one chord of the wing downstream from the wing trailing edge, which coincides with the flow pattern.

Thus, the method of vortex structures visualization of the third generation *Liutex* criterion, due to the fact that it is free from shear and compressive components of the strain rate tensor by its construction, seems promising to the authors for further development and application to vortex structures identification in various flow configurations.

References

1. Wake Turbulence Training Aid (section 2), FAA Report, DOT/FAA/RD-95/6 DOT-VNTSC-FAA-95-4, United States Department of Transportation, 1995.

2. BFU Interim Report BFU17-0024-2X. German Federal Bureau of Aircraft Accident Investigation, 2017.

3. Hansen C.D., Johnson C.R. (Eds.). *The Visualization Handbook*. NY: Academic Press, 2004, 984 p.

4. Chakraborty, P., Balachandar, S., Adrian, R. G. On the relationships between local vortex identification schemes. *J. Fluid Mech.*, **535**, pp 189-214, 2005.

5. Kolář V. Brief Notes on Vortex Identification. *Recent Advances in Fluid Mechanics, Heat and Mass Transfer and Biology* (WSEAS Press, 163 p), pp 23-29, 2011.

6. Volkov K.N. Visualization methods of vertical flows in computational fluid dynamics and their applications. *Scientific and Technical Journal of Information Technologies, Mechanics and Optics*, **91** 3, 2014 (in Russian).

7. Bykov L.V., Molchanov A.M., Scherbakov M.A., Yanyshev D.S. *Computational mechanics of continuous media in problems of aviation and space technology*. LENAND, 2019, 668 p (in Russian).

8. Garbaruk A.V., Strelets M.Kh., Travin A.K., Shur M.L. Modern approaches to the modeling of turbulence. *Manual, Peter the Great St. Petersburg Polytechnic University*, 2016, 233 p (in Russian).

9. V.E. Borisov, A.A. Davydov, I.Yu. Kudryashov, A.E. Lutsky, I.S. Men'shov. Parallel Implementation of an Implicit Scheme Based on the LU-SGS Method for 3D Turbulent Flows. *Mathematical Models and Computer Simulations*, 7(3), p. 222–232, 2015.

10. Borisov V.E., Davydov A.A., Kydryshov I.Yu., Lutsky A.E. ARES software package for numerical simulation of three–dimensional turbulent flows of viscous compressible gas on high-performance computing systems, Certificate of registration of a computer program RU 2019667338, (23 December 2019) (in Russian).

11. Hybrid supercomputer system K-60 https://www.kiam.ru/MVS/resourses/k60.html

12. Jeong J., Hussain F. On the identification of a vortex. *Journal of Fluid Mechanics*, **285**, pp 69–94, 1995.

13. Hunt J.C.R., Wray A.A., Moin P. Eddies, stream, and convergence zones in turbulent flows. *Technical Report* № CTR-S88. Palo Alto: Center for Turbulent Research, pp 193–208, 1988.

14. Liu C., Gao Y., Dong X., Wang Y., Liu J., Zhang Y., Cai X., Gui N. Third generation of vortex identification methods: Omega and Liutex/Rortex based systems. *J. Hydrodyn.*, **31** 2, pp 205–223, 2019.

15. Liu C., Gao Y., Tian S., Dong X. Rortex—A new vortex vector definition and vorticity tensor and vector decompositions. *Phys. Fluids*. 30:035103, 2018.

16. Shrestha P., Nottage C., Yu Y., Alvarez O., Liu C. Stretching and shearing contamination analysis for Liutex and other vortex identification methods. Advances in Aerodynamics. 2021. **3** 8.